Acta Crystallographica Section F
Structural Biology and Crystallization Communications
ISSN 1744-3091

Crystallization and preliminary X-ray diffraction analysis of the truncated cytosolic domain of the iron transporter FeoB

Yaohua Jin,[a,b,c] Motoyuki Hattori,[b,c] Hiroshi Nisimasu,[c] Ryuichiro Ishitani[c] and Osamu Nureki[b,c]*

[a]Department of Chemical Engineering, Tsinghua University, Beijing 100084, People's Republic of China, [b]Department of Biological Information, Graduate School of Bioscience and Biotechnology, Tokyo Institute of Technology, 4259 Nagatsuta-cho, Midori-ku, Yokohama-shi, Kanagawa 226-8501, Japan, and [c]Department of Basic Medical Sciences, Institute of Medical Science, University of Tokyo, 4-6-1 Shirokanedai, Minato-ku, Tokyo 108-8639, Japan

Correspondence e-mail: nureki@ims.u-tokyo.ac.jp

Received 29 December 2008
Accepted 25 June 2009

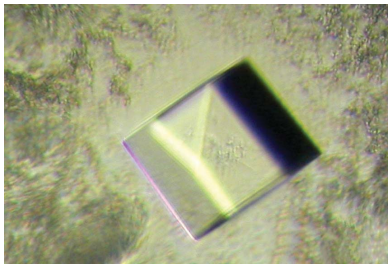

FeoB-family proteins are widely distributed in bacteria and archaea and are involved in high-affinity Fe^{2+} uptake through the plasma membrane. FeoB consists of an N-terminal cytosolic region followed by a C-terminal transmembrane region. The cytosolic region contains small GTPase and GDP dissociation inhibitor-like domains, which serve a regulatory function. The truncated cytosolic region of the iron transporter FeoB from *Thermotoga maritima* was overexpressed, purified and crystallized. Four native or SeMet crystal forms in a nucleotide-free state or in complex with either GDP or GMPPNP diffracted to resolutions of between 1.5 and 2.1 Å.

1. Introduction

Iron is essential for the majority of life and participates in many major biological processes (Andrews *et al.*, 2003). Since both an excess and a deficiency of iron have negative effects, cellular iron homeostasis is critically important. The FeoB-family proteins are widely distributed integral membrane proteins in prokaryotes and are involved in the high-affinity Fe^{2+}-uptake system (Kammler *et al.*, 1993; Cartron *et al.*, 2006). In the pathogen *Helicobacter pylori*, FeoB is essential for the colonization of murine gastric mucosa and therefore provides the major pathway for Fe^{2+} uptake (Velayudhan *et al.*, 2000; Waidner *et al.*, 2002). While the driving force of the transport is still controversial, it has been suggested that FeoB functions as a transport ATPase because Fe^{2+} uptake is inhibited by known ATPase inhibitors such as vanadate (Velayudhan *et al.*, 2000).

Escherichia coli FeoB (GenBank accession No. NP_417868) contains 773 residues and consists of an N-terminal cytosolic domain followed by a C-terminal transmembrane (TM) domain. The N-terminal region of the cytosolic domain has sequence homology to small GTPases, which are well known for their ubiquitous contribution to signal transduction in eukaryotes (Bourne *et al.*, 1990). In contrast, the contribution of bacterial small GTPases to bacterial regulatory pathways is largely unknown (Caldon & March, 2003). The small GTPase domain (G domain) of FeoB hydrolyzes GTP slowly, but is required for Fe^{2+} uptake and has therefore been proposed to serve a regulatory function (Marlovits *et al.*, 2002). Recently, it was revealed that the spacer region (residues 171–274) connecting the G (residues 1–170) and TM (residues 275–773) domains functions as a novel GDP dissociation inhibitor-like (GDI) domain that specifically stabilizes the GDP-binding state of the N-terminal G domain (Eng *et al.*, 2008). Although several structures of bacterial small GTPases have been reported (Chen *et al.*, 1999; Buglino *et al.*, 2002; Scrima *et al.*, 2005), there is no available structural homologue of the FeoB GDI domain. Thus, the mechanism of the GDI function of the FeoB cytosolic domain remains unclear. Here, we report the crystallization and preliminary crystallographic analysis of the truncated cytosolic domain of the iron transporter FeoB from *Thermotoga maritima*.

2. Methods and materials

2.1. Cloning, expression and purification

The domain boundary between the TM and cytosolic domains was predicted using the *PSIPRED* (McGuffin *et al.*, 2000), *TOPPRED* (von Heijne, 1992) and *DISOPRED* (Ward *et al.*, 2004) programs. The truncated cytosolic domain of *T. maritima* FeoB ($TmFeoB_{17–269}$; M_r = 28 655) was cloned from genomic DNA into the *Nde*I and *Bam*HI sites of a pET-28a vector (Novagen, Wisconsin, USA) derivative including an N-terminal hexahistidine tag and a HRV 3C protease site. The recombinant protein was overexpressed in C41 (DE3) (Avidis, Saint-Beauzire, France) *E. coli* cells harbouring pRARE plasmids (Novagen, Wisconsin, USA) encoding rare codons grown in LB medium containing 50 µg ml^{-1} kanamycin at 310 K by induction at an OD_{600} of ∼0.5 with 1 m*M* isopropyl *β*-D-1-thiogalactopyranoside (IPTG) for ∼16 h at 310 K. Selenomethionine-substituted (SeMet) protein was expressed in B834 (DH3) (Novagen, Wisconsin, USA) *E. coli* cells grown in Core medium (Wako, Osaka, Japan) with 50 µg ml^{-1} kanamycin and 25 µg ml^{-1} L-selenomethionine (Nakalai Tesque, Kyoto, Japan) by induction at an OD_{600} of ∼0.5 with 1 m*M* IPTG for 20 h at 310 K. The truncated FeoB cytosolic domain contains five methionines per monomer.

All proteins were purified using the following procedure at 277 K. For all buffers, the pH given refers to that before the inclusion of all ingredients. The *E. coli* cells were disrupted by sonication using a Digital Sonifier (Branson, Connecticut, USA). After sonication in buffer *A* (50 m*M* Tris–HCl pH 8.0, 300 m*M* NaCl and 4 m*M* *β*-mercaptoethanol) containing 1 m*M* PMSF and 20 m*M* imidazole, the disrupted cells were harvested by centrifugation (28 000*g*) for 40 min. *T. maritima* is an extremely thermophilic organism and its proteins are expected to be thermostable. Therefore, the cell lysate was agitated in a heat bath for 15 min at 343 K to remove *E. coli* proteins. After centrifugation (28 000*g*) for 40 min, the supernatant was loaded onto an Ni–NTA agarose column (Qiagen, California, USA) pre-equilibrated in buffer *A* containing 20 m*M* imidazole. The column-bound proteins were washed and eluted in buffer *A* containing 50 and 300 m*M* imidazole, respectively. The N-terminal His_6 tag of the eluted protein was cleaved by HRV3C protease (Takara Bio, Shiga, Japan) for ∼12 h at 310 K during dialysis against 50 m*M* Tris–HCl buffer pH 8.0 containing 50 m*M* NaCl and 4 m*M* *β*-mercaptoethanol. The protease:target protein ratio was 1:100(*w*:*w*). This sample was again applied onto an Ni–NTA column pre-equilibrated with the buffer used for dialysis. The sample contained additional residues (Gly-Pro-Leu-His-Met) at the N-terminus after His-tag digestion. The flowthrough was fractionated and loaded onto a Resource Q 6 ml ion-exchange column (GE Healthcare, New Jersey, USA) pre-equilibrated with 50 m*M* Tris buffer pH 8.0 containing 50 m*M* NaCl and 1 m*M* DTT and the flowthrough was collected. Using an Amicon Ultra 10K filter (Millipore, Massachusetts, USA), the flowthrough was exchanged to 50 m*M* Tris–HCl buffer pH 8.0 containing 50 m*M* NaCl and 5 m*M* EDTA and concentrated. Further purification was carried out on a HiLoad 16/60 Superdex 200 120 ml (GE Healthcare, New Jersey, USA) gel-filtration column in 20 m*M* Tris–HCl buffer pH 8.0 containing 150 m*M* NaCl and 1 m*M* DTT. For crystallization trials, the purified protein was concentrated to approximately 10 mg ml^{-1} using an

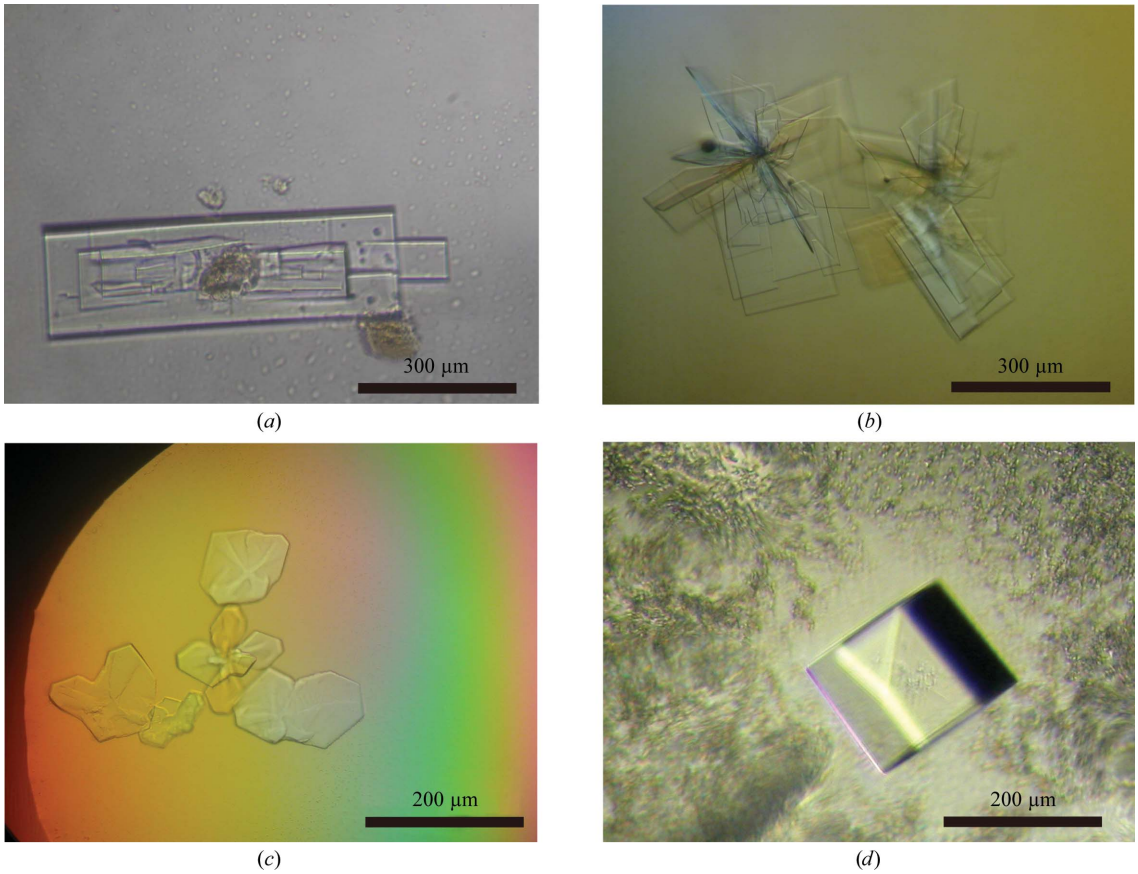

Figure 1
Crystals of the cytosolic domain of *T. maritima* FeoB. (*a*) Form *A*, (*b*) form *B*, (*c*) form C, (*d*) form *D*.

Table 1
Data-collection statistics.

Values in parentheses are for the last shell.

	Form *A*	Form *B*	Form *C*	Form *D*
	SeMet, GDP	Native, GMPPNP	Native, apo	Native, GDP
Wavelength (Å)	0.9718	1.0000	1.0000	1.0000
Crystal-to-detector distance (mm)	406	250	250	142
Space group	$P2_12_12_1$	$P2_1$	$P2_12_12_1$	$P3_12_1$
Unit-cell parameters (Å, °)	a = 46.5, b = 107.2, c = 109.7	a = 43.6, b = 57.3, c = 57.3, α = 90.0, β = 98.0, γ = 90.0	a = 57.4, b = 81.6, c = 128.5	$a = b$ = 65, c = 104.8.2, $\alpha = \beta$ = 90.0, γ = 120.0
Resolution (Å)	50–1.50 (1.53–1.50)	50–1.80 (1.83–1.80)	50–2.10 (2.14–2.10)	50–1.65 (1.68–1.65)
Redundancy†	11.3	3.2	5.6	7.2
Unique reflections	88502	48366	35690	31226
Completeness (%)	99.8 (99.8)	98.1 (93.1)	99.1 (98.4)	98.3 (97.2)
$I/\sigma(I)$	11.4 (2.7)	16.3 (3.4)	10.3 (2.2)	20.7 (2.1)
$R_{\rm merge}$‡	0.077 (0.467)	0.048 (0.223)	0.055 (0.323)	0.045 (0.395)
Matthews coefficient (Å^3 Da^{-1})	2.38	2.36	2.65	2.24
Solvent content (%)	48.5	47.9	53.2	45.1

† Bijvoet pairs were not merged in the calculation of redundancy. ‡ $R_{\rm merge} = \sum_{hkl}\sum_i |I_i(hkl) - \langle I(hkl)\rangle| / \sum_{hkl}\sum_i I_i(hkl)$, where $I_i(hkl)$ is the ith measurement of the intensity of reflection hkl and $\langle I(hkl)\rangle$ is its mean value.

Amicon Ultra 10K filter. The yields of the purified native and SeMet $TmFeoB_{17–269}$ proteins were about 4 and 0.8 mg per litre of culture, respectively.

2.2. Crystallization

We used an IntelliPlate (Art Robbins, California, USA) for initial crystallization screening and a Cryschem plate (Hampton Research, California, USA) for optimization. For crystallization, purified protein solution (10 mg ml^{-1}) was added to each reservoir solution. Initial screening for crystallization conditions was performed using Crystal Screen I, Crystal Screen II, Natrix, MembFac, Index Screen and SaltRX kits (Hampton Research, California, USA), JB Screen kits (Jena Bioscience, Jena, Germany) and MemSys and MemStart kits (Molecular Dimensions, Suffolk, England). A Hydra II Plus One crystallization robot (Matrix Technologies, New Hampshire, USA) was used for the initial crystallization screen, which used the sitting-drop vapour-diffusion method at 293 K. Crystallization drops prepared by mixing 0.2 µl protein solution and 0.2 µl reservoir solution were equilibrated against 100 µl reservoir solution. Prior to crystallization experiments, 500 m*M* $MgCl_2$ and either 100 m*M* GDP (Sigma, St Louis, USA) or 100 m*M* GMPPNP (GNPl Sigma, St Louis, USA) were optionally added to the protein solution. These solutions were added to the protein solution so that the final concentrations of $MgCl_2$ and nucleotides were 5 and 1 m*M*, respectively.

Native and SeMet crystals of $TmFeoB_{17–269}$ in the presence and absence of GDP or GMPPNP were first obtained in a week from condition No. 35 of Crystal Screen II (Hampton Research, California, USA). Further crystals in the presence of GDP were obtained under condition No. 73 of Index Screen (Hampton Research, California, USA). To optimize the crystallization conditions, crystallization drops prepared by mixing 1 µl protein solution and 1 µl reservoir solution were equilibrated against 500 µl reservoir solution. SeMet crystals in the presence of GDP were obtained under a condition containing 60–64% 2-methyl-2,4-pentanediol (MPD), 0.1 *M* HEPES pH 7.5 (Fig. 1*a*; crystal form *A*). Native crystals in the presence of GMPPNP were obtained under a condition containing 60–66% MPD, 0.1 *M* HEPES pH 7.5 and 4% 1,3-butanediol (Fig. 1*b*; crystal form *B*). Native crystals in the absence of GMPPNP or GDP were obtained under a condition containing 62–64% MPD and 0.1 *M* HEPES pH 7.5 (Fig. 1*c*; crystal form *C*). Native crystals in the presence of GDP were obtained under a condition containing 25% PEG 3350, 0.1 *M* Tris–HCl pH 8.5 and 0.1 *M* NaCl (Fig. 1*d*; crystal form *D*). For observation of crystals, we used an Eclipse 50i POL (Nikon, Tokyo, Japan) without polarized light.

2.3. Preliminary crystallographic analysis

X-ray diffraction data sets were collected at 100 K under a cold nitrogen stream with an oscillation range per image of 1° using an ADSC Quantum 315 detector on beamline BL41XU at SPring-8 (Harima, Japan) or an ADSC Quantum 210 detector on beamline NW12 at Photon Factory (Tsukuba, Japan). All diffraction data sets were processed using the programs *DENZO* and *SCALEPACK* (Otwinowski & Minor, 1997) and the *CCP*4 suite (Collaborative Computational Project, Number 4, 1994). SeMet crystals of form *A* could be frozen directly in liquid nitrogen, while crystals of forms *B*, *C* and *D* were directly transferred into cryoprotectant solutions containing 40% MPD and 0.1 *M* HEPES pH 7.0, 5 m*M* $MgCl_2$ and 1 m*M* GMPPNP (form *B*), containing 40% MPD and 0.1 *M* HEPES pH 7.0 (form *C*) and containing 25%(*w*/*v*) PEG 3350, 0.1 *M* Tris–HCl pH 8.5, 0.1 *M* NaCl, 5 m*M* $MgCl_2$, 1 m*M* GDP and 30% glycerol (form *D*). The Matthews coefficients and solvent contents were calculated using *CCP*4 (Collaborative Computational Project 4, Number 4, 1994). The heavy-atom sites were identified using the program *SHELXD* (Sheldrick, 2008).

3. Results and discussion

We first attempted to crystallize the entire TmFeoB cytosolic domain (residues 1–288). The domain boundary between the cytosolic (residues 1–286) and TM (residues 287–669) domains was predicted using the *PSIPRED* (McGuffin *et al.*, 2000) and *TOPPRED* (von Heijne, 1992) programs. However, no well diffracting crystals were obtained in the presence or the absence of nucleotides. The N-terminal and C-terminal regions of the cytosolic domain (1–288) were predicted to be disordered by *DISOPRED* (Ward *et al.*, 2004). Thus, we attempted the crystallization of a truncated region (17–269) of the TmFeoB cytosolic domain. As a result, we successfully obtained well diffracting crystals of the TmFeoB cytosolic domain in the presence and absence of nucleotides. We could not harvest crystals of forms *B* and *C* without reducing the MPD concentration. Using a harvest buffer containing over 60% MPD, the crystals were easily dissolved. The data-collection statistics are summarized in Table 1. Considering the general range of Matthews coefficients observed for protein crystals (1.6–4.0 Å^3 Da^{-1}; Matthews, 1968), crystal forms *A*, *B* and *C*

contained two molecules in the asymmetric unit, while crystal form *D* contained one molecule in the asymmetric unit.

The molecular weight of the truncated FeoB cytosolic domain estimated by gel filtration using gel-filtration standards (Bio-Rad, California, USA) was 38 kDa, which is significantly lower than the molecular mass of the dimer (58 kDa; data not shown). Therefore, the FeoB cytosolic domain is most likely to be a monomer in solution. We have already identified ten selenium sites using the program *SHELXD* (Sheldrick, 2008). The number of selenium sites is equivalent to that for two $TmFeoB_{17–269}$ molecules, which is reasonably consistent with the Matthews coefficient of crystal form *A*. Structure determination is in progress.

We thank the beamline staff at the BL41XU station of SPring-8 (Harima, Japan) and at the NW12 station of Photon Factory (Tsukuba, Japan) for technical help during data collection. This work was supported by a PRESTO Program grant from JST (Japan Science and Technology) to ON and by grants from MEXT to ON and RI.

References

Andrews, S. C., Robinson, A. K. & Rodriguez-Quinones, F. (2003). *FEMS Microbiol. Rev.* **27**, 215–237.
Bourne, H. R., Sanders, D. A. & McCormick, F. (1990). *Nature (London)*, **348**, 125–132.
Buglino, J., Shen, V., Hakimian, P. & Lima, C. D. (2002). *Structure*, **10**, 1581–1592.
Caldon, C. E. & March, P. E. (2003). *Curr. Opin. Microbiol.* **6**, 135–139.
Cartron, M. L., Maddocks, S., Gillingham, P., Craven, C. J. & Andrews, S. C. (2006). *Biometals*, **19**, 143–157.
Chen, X., Court, D. L. & Ji, X. (1999). *Proc. Natl Acad. Sci. USA*, **96**, 8396–8401.
Collaborative Computational Project, Number 4 (1994). *Acta Cryst.* D**50**, 760–763.
Eng, E. T., Jalilian, A. R., Spasov, K. A. & Unger, V. M. (2008). *J. Mol. Biol.* **375**, 1086–1097.
Heijne, G. von (1992). *J. Mol. Biol.* **225**, 487–494.
Kammler, M., Schon, C. & Hantke, K. (1993). *J. Bacteriol.* **175**, 6212–6219.
Marlovits, T. C., Haase, W., Herrmann, C., Aller, S. G. & Unger, V. M. (2002). *Proc. Natl Acad. Sci. USA*, **99**, 16243–16248.
Matthews, B. W. (1968). *J. Mol. Biol.* **33**, 491–497.
McGuffin, L. J., Bryson, K. & Jones, D. T. (2000). *Bioinformatics*, **16**, 404–405.
Otwinowski, Z. & Minor, W. (1997). *Methods Enzymol.* **276**, 307–326.
Scrima, A., Vetter, I. R., Armengod, M. E. & Wittinghofer, A. (2005). *EMBO J.* **24**, 23–33.
Sheldrick, G. M. (2008). *Acta Cryst.* A**64**, 112–122.
Velayudhan, J., Hughes, N. J., McColm, A. A., Bagshaw, J., Clayton, C. L., Andrews, S. C. & Kelly, D. J. (2000). *Mol. Microbiol.* **37**, 274–286.
Waidner, B., Greiner, S., Odenbreit, S., Kavermann, H., Velayudhan, J., Stahler, F., Guhl, J., Bisse, E., van Vliet, A. H., Andrews, S. C., Kusters, J. G., Kelly, D. J., Haas, R., Kist, M. & Bereswill, S. (2002). *Infect. Immun.* **70**, 3923–3929.
Ward, J. J., McGuffin, L. J., Bryson, K., Buxton, B. F. & Jones, D. T. (2004). *Bioinformatics*, **20**, 2138–2139.